IEEE Access
Multidisciplinary | Rapid Review | Open Access Journal

Received February 9, 2022, accepted March 4, 2022, date of publication March 10, 2022, date of current version March 22, 2022.

Digital Object Identifier 10.1109/ACCESS.2022.3158485

Evaluation Analysis on Leakage Performance for Beam Seal With Two Sealing Areas

YINGJIA YU[1], YING CUI[1], HONGXIANG ZHANG[1], DAWEI WANG[1], AND JINGJUN ZHONG[2]
[1]Naval Architecture and Ocean Engineering College, Dalian Maritime University, Dalian, Liaoning 116026, China
[2]Merchant Marine College, Shanghai Maritime University, Shanghai 210306, China

Corresponding author: Ying Cui (cuiying@dlmu.edu.cn)

This work was supported in part by the Fundamental Research Funds for the Central Universities under Grant 3132017007.

ABSTRACT As a special type of aviation hydraulic pipe joint, a beam seal comprises two annular sealing areas. This paper presented a leakage model for an annular sealing area based on a developed three-dimensional percolation grid model and the porous medium theory. Both average contact pressure and true contact width of the beam seal were simulated using the finite element method. An experimental study of beam seal verified the accuracy of the numerical results. Considering that the two sealing areas and the groove in the beam seal form an isolated sealing system, a leakage model of the beam seal is proposed based on the leakage model for annular sealing area. We evaluated the effects of the roughness of the surface, preload and fluid pressure on the leak rate of the beam seal. Furthermore, the geometry of the beam seal was modified to improve its sealing performance. This study provides an evaluation method for optimizing the design and improving the sealing performance of the beam seal.

INDEX TERMS Beam seal, sealing performance, three-dimensional percolation grid model, porous medium, leakage model.

I. INTRODUCTION

Aviation hydraulic pipe joints are basic hydraulic accessories that combine hydraulic pumps, valves, cylinders, and other hydraulic components through pipes to form a hydraulic system. Pipe joints are widely distributed in aircraft hydraulic systems, and any leakage of pipe joints will cause the aircraft hydraulic system to malfunction. Among these pipe joints, the beam seal, as a new type of seal, can form two annular sealing areas during the assembly. Accordingly, the beam seal has a higher sealing performance than conical and ball-head seals. For the beam seal, the allowable fluid pressure ranges from 22.7 MPa to 55.2 MPa, and it can withstand severe vibration and high-pressure pulsation. Moreover, the beam seal can be assembled and disassembled more than 25 times without leakage [1], [2]. Owing to these advantages, the beam seal is expected to replace the aviation hydraulic pipe joints currently used.

At present, most of the information about beam seal comes from the SAE standards [3]–[5]. There are few reports on the theoretical research of beam seals, much less on the evaluation analysis of the leakage performance of the beam seal.

The associate editor coordinating the review of this manuscript and approving it for publication was Jingang Jiang.

For a main interface docking (MID) seal with two sealing areas, Liao *et al.* [6] predicted the leak rate of gas at the sealing interface based on the theory of porous media, and the leakage property of the MID seal was studied by considering the primary and secondary seals as a whole. The research method in this article provides a new perspective for the study of seals consisting of two sealing areas. Moreover, it proves that predicting the leakage of the sealing interface is essential for evaluating the sealing property of the seal. However, the leak rate prediction method for the sealing interface is only suitable for rubber seals, and the three-dimensional characteristics of porous media are not considered when calculating the leak rate of sealing interface.

In recent years, some progress has been made in the prediction of the leakage of sealing interface. Persson *et al.* [7], [8] simplified the sealing interface into a two-dimensional percolation grid model to explore the sealing mechanism and proposed a leakage model. The basic idea is that the contact area and non-contact area on the sealing interface are regarded as black and white clusters respectively, and the clusters of these two colors form a two-dimensional percolation grid model. As the magnification increased, the number of white clusters gradually increased. When the white clusters penetrate the sealing interface, the white clusters at this time are defined

as the critical leakage channel and the leakage is calculated. Lorenz and Perrson compared the theoretically calculated leakage with the experimentally measured leakage to verify the accuracy of sealing theory [9]. Akulichev *et al.* [10] used Perrson's leakage model and finite element analysis to predict the seal failure temperature of O-ring seal. However, Bottiglione pointed out that the selection of parameter l/L (the ratio of sealing interface transversal length to longitudinal length) in Perrson's model would cause prediction uncertainty of the leak rate, and a better estimation of the cross-sectional height of the leakage channel should consider the real separation between the two sealing surfaces [11].

Meanwhile, some scholars have regarded the sealing interface as a porous medium to calculate the leakage of the sealing interface. Kazeminia *et al.* proposed that the porous media theory is an attractive method that can be used to predict leak rates through the sealing interface [12]. Considering a sealing interface consisting of a rigid plane and a rough surface, Sun *et al.* calculated the initial porosity and built a novel leakage channel model based on fractal theory and the two-dimensional percolation grid model [13]. Referring to Sun's leakage channel construction method, Ni *et al.* applied fractal theory and Hagen Poiseuille's equation to establish a leakage model, and studied the effect of fractal dimension on leakage [14]. Furthermore, Zhang *et al.* [15] obtained the permeability of the sealing interface based on porous medium and fractal theory, and a sealing interface leakage model was established by applying Darcy's law instead of constructing the leakage channel. Zhang *et al.* [16] compared experimental results with numerical simulation results and proved that the leakage model could accurately predict the leakage on the surface with fractal characteristics. However, there is a large discrepancy in the leakage prediction on a surface that does not conform to the fractal feature or that is an anisotropic surface. These studies show that the two-dimensional percolation grid model and porous media theory are effective methods for studying the leakage problems of rough interfaces, and provide useful references for the evaluation analysis of the leakage performance of the beam seal.

In this study, we aimed to develop a leakage model to evaluate the sealing performance of a beam seal with two annular sealing areas and to modify the geometry of the beam seal. Considering that the sealing interface consists of two rough surfaces, a three-dimensional percolation grid model was proposed to simulate the sealing interface, and the porosity was calculated. Subsequently, a leakage model of an annular sealing area is established by combining the three-dimensional percolation grid model with percolation mechanics. An elastic-plastic finite element contact model of the beam seal was developed, and a test rig was built to verify the effectiveness of the finite element calculation results. Furthermore, a leakage model of the beam seal is proposed by combining the macro-contact analysis of the beam seal with the annular sealing area leakage model, and the leakage characteristics are studied. Based on the leakage characteristics of the beam seal, the geometry of the existing beam seal was modified to improve the sealing performance.

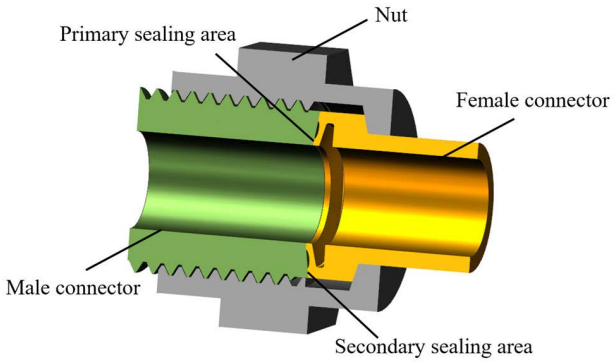

FIGURE 1. Schematic view of beam seal.

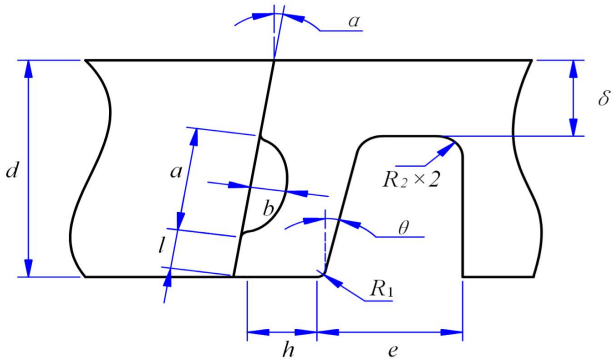

FIGURE 2. Parameterization of female connector.

II. CONFIGURATION AND PAREMETERIZATION OF BEAM SEAL

The beam seal consists of female connector, male connector, and nut, as illustrated in Fig.1 [5]. The main sealing component of the beam seal is the female connector, whose geometrical characteristics are the U-section and the oval-arc groove on the sealing beam. The groove divides the sealing surface into two areas, one is the primary sealing area near the inner side, and the other is the secondary sealing area near the outer side.

The geometrical parameters of the female connector are shown in Fig.2, d is wall thickness of male connector, a is major axis of elliptical groove, R_1 or R_2 is radius of rounded corner, b is minor axis of elliptical groove, δ is distance between bottom of U-shaped and outer diameter of female connector, α is taper angle, e is axial length of U-shaped port, θ is inclined angle of U-shaped section, h is seal beam section width, l is nominal contact width of the primary seal. In order to study the leakage characteristics of the beam seal, it is necessary to establish a leakage model for the annular sealing area.

III. LEAKAGE MODEL OF THE ANNULAR SEALING AREA

To comprehensively consider the surface topography of the two sealing surfaces, inspired by the two-dimensional percolation grid model, a three-dimensional percolation grid model

was proposed based on point cloud data, and the porosity was derived using the porous media theory.

A. NUMERICAL SIMULATION OF ROUGH SURFACE

The characterization of the topography of the sealing surface is the basis of contact mechanics and sealing performance analysis. In this study, the autocorrelation function method was used to simulate the topography of a rough surface [17]. The exponential autocorrelation function is expressed as follows:

$$F(x, y) = \sigma_s \exp\{-2.3 \times [(\frac{x}{\beta_x})^2 + (\frac{y}{\beta_y})^2]^{\frac{1}{2}}\} \quad (1)$$

where σ_s is the root mean square roughness; β_x and β_y are the autocorrelations of the x and y directions, respectively. The values of β_x and β_y reflect the fluctuation frequency of a rough surface. If β_x and β_y are equal, the rough surface is isotropic; otherwise, it is anisotropic. This paper mainly discusses isotropic rough surfaces. The point cloud data and contour of the rough surface are shown in Fig.3.

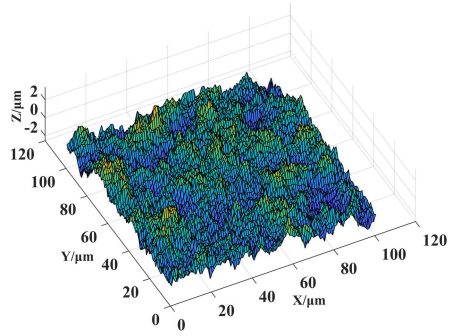

(a)Point cloud data of rough surface with σ_s=0.4,β_x=β_y=10

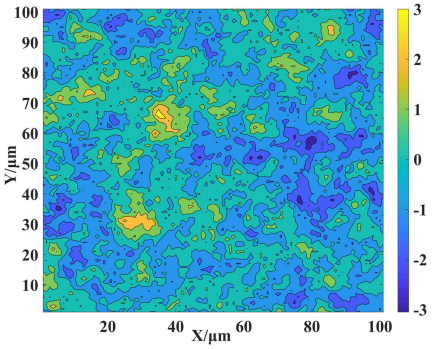

(b)Contour of rough surface with σ_s=0.4, β_x=β_y=10

FIGURE 3. Numerical simulation of sealing surface.

B. THREE-DIMENSIONAL PERCOLATION GRID MODEL AND CALCULATION OF POROSITY

Porosity and permeability are important factors that affect leakage [12]. To calculate the porosity of the sealing interface accurately, the sealing surface was discretized into a large number of columns. The number of columns depended on the number of points and the height of each column corresponded to the point cloud data. Based on the point cloud data, a three-dimensional percolation grid model of the sealing interface is shown in Fig. 4.

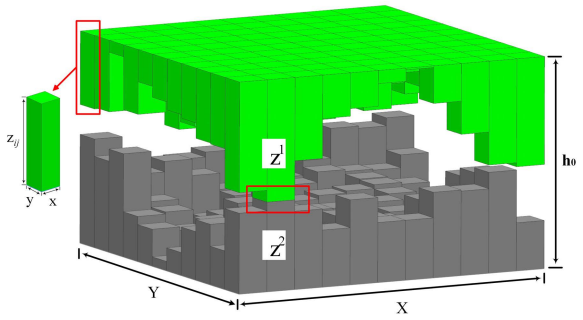

FIGURE 4. The three-dimensional percolation grid model of sealing interface.

When the two sealing surfaces are in contact for the first time, the initial porosity $\phi(0)$ is:

$$\phi(0) = 1 - \frac{V_{solid}}{V_0} = 1 - \frac{xy\sum_{i=1}^{n}\sum_{j=1}^{n}(z_{ij}^1 + z_{ij}^2)}{XYh_0} = 1 - \frac{\sum_{i=1}^{n}\sum_{j=1}^{n}(z_{ij}^1 + z_{ij}^2)}{Nh_0} \quad (2)$$

where V_0 is the initial volume of the sealing interface, V_{solid} is the volume of the skeleton, N is the number of columns on the sealing surface, x is the length of the column, and y is the width of the column. The height matrix of the upper sealing surface is z^1, the height matrix of the lower sealing surface is z^2. n is the number of columns in the X-direction, which is equal to the number of columns in the Y-direction. The critical height of the two roughness surfaces h_0 is:

$$h_0 = \max(z_{ij}^1 + z_{ij}^2) \quad (3)$$

From equation (3), it can be seen that the critical height is related to the surface topography, and the critical height is proportional to σ_s. When the upper sealing surface moves downward, the interference is ω, and the height of the sealing interface decreases from h_0 to h_0-ω. Consequently, the V_0will change to be $XY(h_0$-$\omega)$ and V_{solid} remains constant [11]. Therefore, the corresponding porosity $\phi(\omega)$ is:

$$\phi(\omega) = \frac{XY(h_0 - \omega) - [(1 - \phi(0)]XYh_0}{XY(h_0 - \omega)} = 1 - \frac{[(1 - \phi(0)]h_0}{h_0 - \omega} \quad (4)$$

where: ω is proportional to the average contact pressure P_t, which can be obtained using the ZMC contact model [18]:

$$P_t(\omega) = \frac{4}{3}\eta E^* R^{1/2} \int_g^{g+\omega_a} \omega^{3/2}\Phi(z)\,dz + \pi RH\eta \int_{g+\omega_a}^{g+\omega_b} \times \left\{0.4\left(\frac{\omega}{\omega_a}\right)^{1/2}[1 - f(\omega)] + f(\omega)\right\} \times [1 + f(\omega)]\,\omega\Phi(z)\,dz + 2\pi\eta HR \int_{g+\omega_b}^{\infty} \omega\Phi(z)\,dz \quad (5)$$

The ZMC contact model is suitable for calculating contact pressure of sealing interface under light load, moderate load and heavy load. Where: E^* is equivalent elastic modulus; R is radius of curvature of an asperity; η is areal density of asperities; H is material hardness; $\Phi(z)$ is gaussian distribution function of asperity heights. g is the mean separation between the two surfaces; ω_a is critical interference at the point of initial yield; ω_b is critical interference at the point of fully plastic flow. The Eq. (4) is applicable to calculate the porosity of isotropic surfaces. According to Eqs. (4) and (5), we can obtain the porosity of sealing interface corresponding to average contact pressure.

C. CALCULATION OF PERMEABILITY AND LEAKAGE MODEL OF THE ANNULAR SEALING AREA

The permeability reflects the seepage capacity of porous media. A study on the flow of single-phase Newtonian fluids in porous media showed that the permeability K is only related to the structural characteristics of porous media. The expression for K is as follows:

$$k = \frac{c\phi^3}{\tau(\frac{1.896}{R})^2} \tag{6}$$

where: c is the Kozeny-Carman constant, which is a constant between 5 and 6, and τ is the tortuosity. According to the literature [15], the expression for tortuosity is:

$$\tau = \frac{1}{2}[1 + \frac{1}{2}\sqrt{1-\phi} + \sqrt{1-\phi}\frac{\sqrt{(\frac{1}{\sqrt{1-\phi}} - 1)^2 + \frac{1}{4}}}{1-\sqrt{1-\phi}}] \tag{7}$$

Combining Eqs. (2), (3), (4), (5) and (7) with Eq. (6), the permeability of porous media corresponding to different average contact pressures is obtained, and the permeability is inversely proportional to average contact pressure.

An annular sealing area with an outer diameter of R and inner diameter of r is taken as the research object. Assuming that the fluid pressure at the inner diameter is P_{in}, and the external environment pressure is P_{o}, the fluid leaks from the inside to the environment. According to reference [15], the equation for the leak rate Q is as follows:

$$Q = -2\pi\,(h_0 - \omega)\,\frac{K\,(\omega)}{\mu}\,\frac{P_{in} - P_o}{\ln\frac{R}{r}} \tag{8}$$

where: the negative sign in the Eq. 8 represents leakage, μ is the fluid viscosity. We can use the annular sealing area leakage model to analyze the leakage characteristics of the beam seal.

IV. CONTACT ANALYSIS AND LEAKAGE MODEL OF THE BEAM SEAL

For the fact that the leakage of the beam seal is affected by the macroscopic geometry and the microtopography of the sealing surface. Therefore, a macro finite element model of the beam seal was established and simulated to calculate the average contact pressure and true contact width on the two seals. A leakage model of the beam seal was developed by combining the macroscopic analysis of the beam seal with the leakage model of the annular sealing area.

A. MACRO FINITE ELEMENT ANALYSIS OF BEAM SEAL AND EXPERIMENTAL VERIFICATION

The geometrical parameters of the beam seal that are suitable for a pipe with a diameter of 12 mm are listed in Table 1.

TABLE 1. Geometrical parameters of beam seal.

Parameter	Value	Parameter	Value
d	2.7 mm	a	1.78 mm
R_1,R_2	0.1,0.3 mm	b	0.3 mm
δ	1.4 mm	α	8.5°
e	1.1 mm	θ	15°
h	0.6 mm	l	0.57 mm

The Abaqus software is used to establish the finite element contact model of the beam seal, as shown in Fig.5. The material is stainless steel, its elastic modulus E is 210GPa, and Poisson's ratio ν is 0.3. The plastic constitutive relations of the stainless steel are shown in Table 2.

TABLE 2. The plastic constitutive relations.

Real stress	Plastic strain	Real stress	Plastic strain
500 MPa	0	882 MPa	0.25
605 MPa	0.029	921 MPa	0.45
695 MPa	0.056	988 MPa	0.75
780 MPa	0.095	1110 MPa	0.85

The sealing surface of female connector is defined as the main contact surface, and the sealing surface of male connector is defined as slave contact surface. Subsequently, the finite slip formula was used to constrain the two contact surfaces. To simulate the connection of the nut to the beam seal, a reference point RP-1 was created at the nut position, and the distributed coupling constraint was applied to connect RP-1 with the female connector. A fixed constraint was applied at the bottom of the male connector based on the actual force of the beam seal, and a preload was applied to the reference point RP-1. The CAX4I element was used to mesh the beam seal, and the number of elements was 23102.

Applying a 1000N preload to the beam seal, the contour of the contact pressure is shown in Fig.6(a). The true contact width of the primary seal is 0.11mm and that of the secondary seal is 0.43 mm. It is evident that the true contact width of the primary seal is less than the average contact width l, the primary seal after assembly is warped and deformed, as shown in Fig.6(b).

To verify the accuracy of the finite element analysis of the beam seal, we machined a male connector and a female connector. Taking the true contact width as the contrast index, the experiment was conducted using the test rig, as shown in Fig.7. The preload part was assembled with a female connector to exert the preload on the beam seal, and the value of the preload was measured using a pressure sensor. To accurately measure the true contact width on the sealing surface, a high-precision Fuji pressure-sensitive test film was placed on the mating surfaces of the male and female connectors,

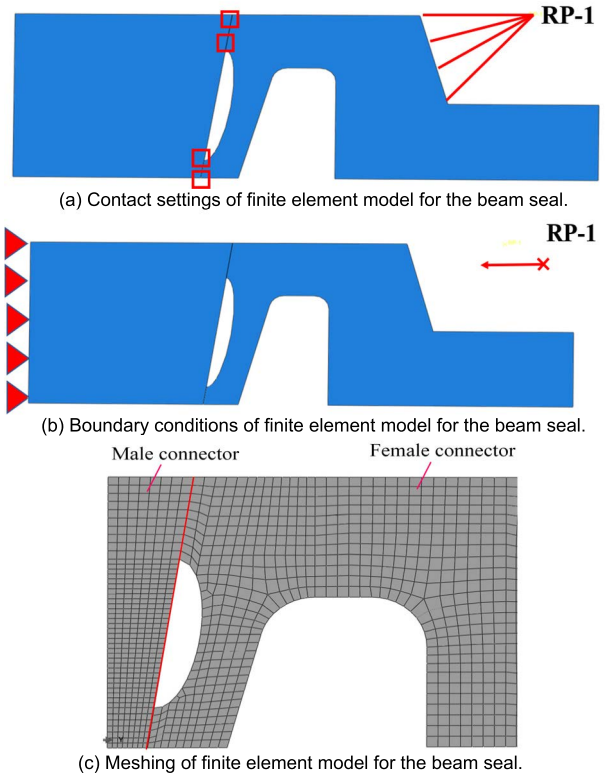

(a) Contact settings of finite element model for the beam seal.

(b) Boundary conditions of finite element model for the beam seal.

(c) Meshing of finite element model for the beam seal.

FIGURE 5. Finite element model of beam seal.

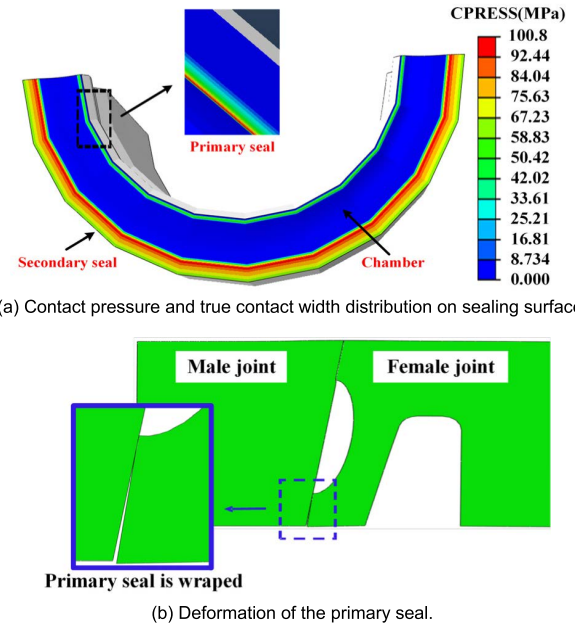

(a) Contact pressure and true contact width distribution on sealing surface.

(b) Deformation of the primary seal.

FIGURE 6. Finite element calculation results.

as shown in Fig.8. Under the condition of 1000N preload, the experimental results of Fuji test film are shown in Fig.9. The UG software was used to measure the color width of the films.

A comparison between the experimental and finite element results is shown in Fig.10. It can be observed that the experimental results are in good agreement with the data of the finite element calculation, which verifies the accuracy of the finite element analysis of the beam seal. The experimental results

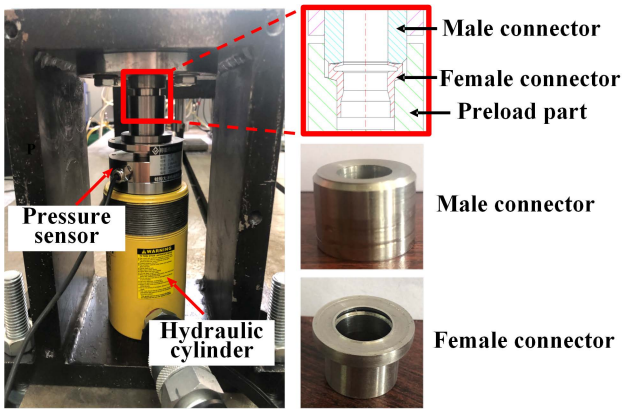

FIGURE 7. Photograph of the test rig.

were slightly larger than the finite element results due to the pigment overflows during the pressure-sensitive test film is squeezed.

B. LEAKAGE MODEL OF BEAM SEAL

A beam seal forms two annular sealing areas. Owing to its geometry, the two seals and groove form an isolated sealing system. The sealing principle is illustrated in Fig.11.

The process of the fluid flowing to the external environment through the beam seal can be divided into three stages: (1) During assembly of beam seal, the groove is filled air with atmospheric pressure; (2) Driven by the fluid pressure in the pipe, the fluid flows into the groove through the primary seal. With the inflow of fluid, the air in the groove is gradually compressed; (3) When the pressure in the groove reaches pressure P_g, the fluid leaks to the external environment through the secondary seal, and finally reaches the equilibrium state. It can be seen that the P_g is the pressure driving fluid leakage, which we define as effective pressure.

Under the equilibrium condition, the effective pressure in the groove remains constant. According to the conservation of mass theorem, the inlet flow of the primary seal is equal to the outlet flow of the secondary seal, which is expressed as follows:

$$2\pi\left(h_0-\omega_1\right)\frac{K\left(\omega_1\right)}{\mu}\frac{P_{in}-P_g}{\ln\frac{R^1}{r^1}}=2\pi\left(h_0-\omega_2\right)\frac{K\left(\omega_2\right)}{\mu}\frac{P_g-P_o}{\ln\frac{R^2}{r^2}} \tag{9}$$

where ω_1 denotes the interference of the primary seal, R^1 and r^1 are the outer and inner diameter of the primary seal, respectively; ω_2 denotes the interference of the secondary seal, R^2 and r^2 are the outer and inner diameter of the secondary seal, respectively; P_{in} denotes the fluid pressure in the pipe. The effective pressure can be derived from Eq. (9), and shown as:

$$P_g=\frac{P_{in}\left(h_0-\omega_1\right)K\left(\omega_1\right)\ln\frac{R^2}{r^2}+P_o\left(h_0-\omega_2\right)K\left(\omega_2\right)\ln\frac{R^1}{r^1}}{\left(h_0-\omega_2\right)K\left(\omega_2\right)\ln\frac{R^1}{r^1}+\left(h_0-\omega_1\right)K\left(\omega_1\right)\ln\frac{R^2}{r^2}} \tag{10}$$

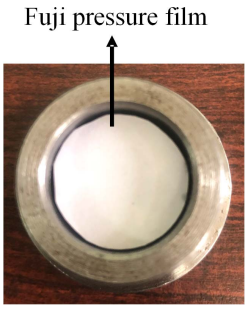

FIGURE 8. Photograph of pressure sensitive test film.

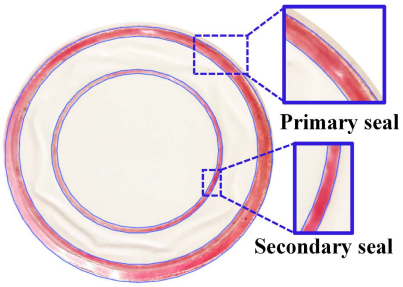

FIGURE 9. Measurement results of the pressure sensitive test film.

Assuming the external environment pressure $P_o = 0$, the depressurization ratio of the effective pressure to the fluid pressure in the pipe can be derived from Eq. (10), and shown as:

$$\frac{P_g}{P_{in}} = 1 - \frac{(h_0 - \omega_2)\, K\,(\omega_2) \ln \frac{R^1}{r^1}}{(h_0 - \omega_1)\, K\,(\omega_1) \ln \frac{R^2}{r^2} + (h_0 - \omega_2)\, K\,(\omega_2) \ln \frac{R^1}{r^1}} \tag{11}$$

The expression of leakage for the secondary seal:

$$Q = 2\pi\,(h_0 - \omega_2)\,\frac{K\,(\omega_2)}{\mu}\,\frac{P_g}{\ln \frac{R^2}{r^2}} \tag{12}$$

The leakage of the beam seal is finally obtained by substituting the expression of P_g into Eq. (12), and it becomes:

$$Q = \frac{2\pi}{\mu} \cdot \frac{P_{in}}{\frac{\ln R^1/r^1}{(h_0-\omega_1)} \cdot \frac{1}{K(\omega_1)} + \frac{\ln R^2/r^2}{(h_0-\omega_2)} \cdot \frac{1}{K(\omega_2)}} \tag{13}$$

V. RESULTS AND DISCUSSION

The beam seal suitable for a pipe with diameter of 12 mm was taken as the research object, and its structural parameters are shown in Table 1. Its material was a stainless steel with hardness H= 850MPa. According to the macro finite element analysis of the beam seal, the average contact pressure and true contact width of the two sealing areas under different preload can be obtained. Subsequently, the proposed leakage model can be used to evaluate the effects of the surface, preload and fluid pressure in the pipe on the leakage performance of the beam seal.

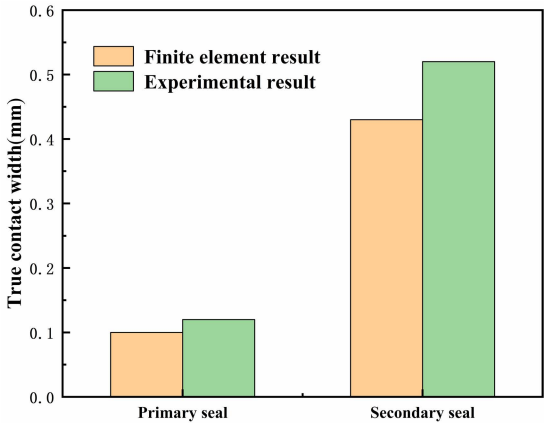

FIGURE 10. Experimental and predicted true contact width.

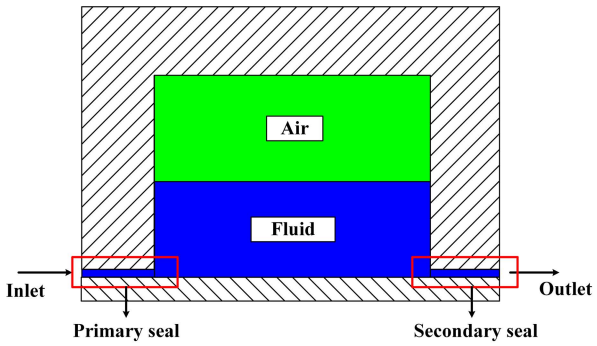

FIGURE 11. Sketch of isolated sealing system for beam seal.

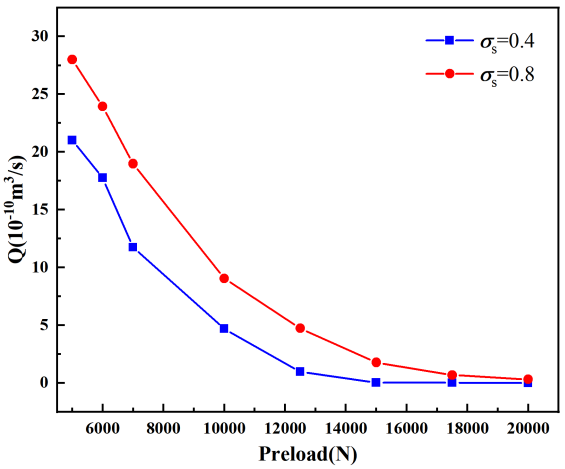

FIGURE 12. The leak rate versus preload with σs=0.4 and σs=0.8.

A. EFFECTS OF SURFACE ROUGHNESS AND PRELOAD ON LEAKAGE OF BEAM SEAL

The point cloud data of sealing surfaces with $\sigma_s = 0.4$ and $\sigma_s = 0.8$ are obtained by using Eq. (1). The viscosity of the fluid in the pipe is set to 0.02Pa.s, the fluid pressure in pipe is 50MPa. We calculated the leakage of beam seal with the two kinds of surface roughness. Fig.12 shows that with the increase of preload, the leakage of the beam seal decreases rapidly, and the leakage of surface with $\sigma_s = 0.4$ is less than that of surface with $\sigma_s = 0.8$. It is indicated that

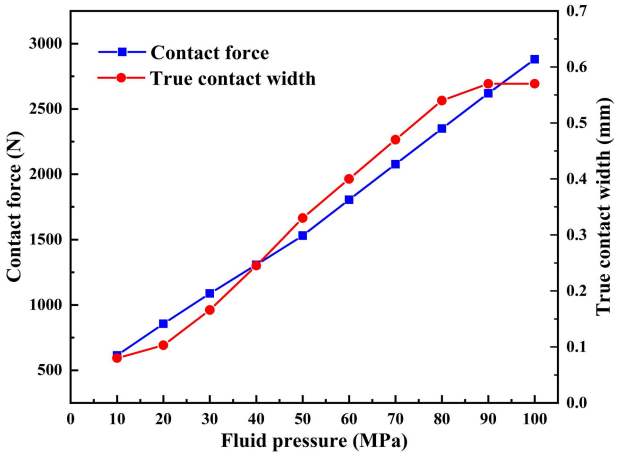

FIGURE 13. Contact force and true contact width of primary seal.

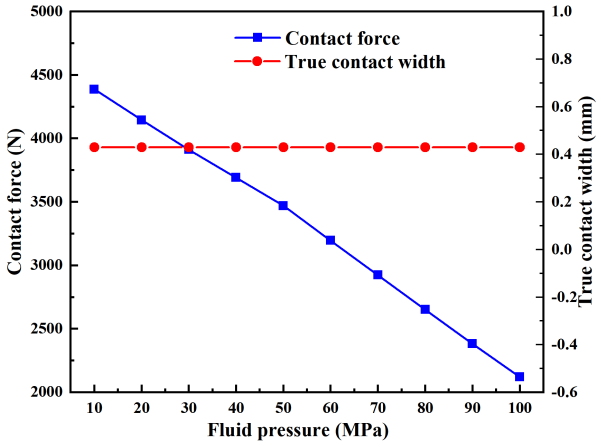

FIGURE 14. Contact force and true contact width of secondary seal.

reducing roughness of the contact surface can improve the sealing performance of beam seal.

B. EFFECT OF FLUID PRESSURE ON SEALING PERFORMANCE OF BEAM SEAL

Effective pressure is one of the key factors to evaluate the sealing performance of beam seal. From Eq. (11), the depressurization ratio is less than 1, which means that the effective pressure of beam seal is less than the fluid pressure in the pipe. In comparison, for the traditional pipe joints with one sealing area, effective pressure is equal to the fluid pressure in pipe. Obviously, the isolation sealing system can reduce the pressure driving the leak, the sealing performance of beam seal is better than that of traditional pipe joint.

To examine the effect of fluid pressure on the sealing performance, the fluid pressure ranging from 10MPa to 100MPa is applied to the beam seal, the roughness of the sealing surface is 0.4, and the preload is set to 5000N. The contact force and true contact width of primary seal versus fluid pressure are shown in Fig.13. The contact force of the primary seal is proportional to the fluid pressure. This phenomenon indicates that the fluid pressure in the pipe exerts additional pressure on the primary seal, which is beneficial to improve

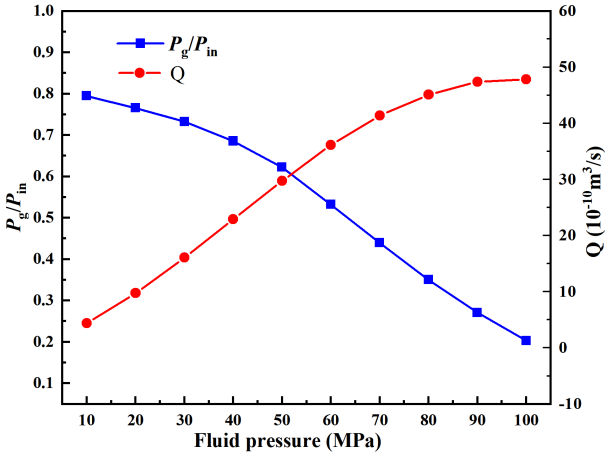

FIGURE 15. Leak rate and depressurization ratio versus fluid pressure.

the sealing performance. The trend of true contact width is the same as that of contact force. This is because the primary seal after assembly is warped and deformed, and the uncontacted sealing surface of the primary seal is gradually compressed under the action of fluid pressure, resulting in a gradual increase in true contact band.

Fig.14 shows the contact force and true contact width of the secondary seal versus fluid pressure. The contact force decreases linearly with the increase of fluid pressure, while the contact width remains constant. This makes the average contact pressure of the secondary seal decrease with the increase of fluid pressure, which leads to an increase in permeability of the secondary seal $K(\omega_2)$.

We calculated the change of leakage rate and depressurization ratio with the fluid pressure, as shown in Fig.15. The depressurization ratio is inversely proportional to fluid pressure, and the leakage rate is proportional to fluid pressure. Fig.15 demonstrates that the beam seal did not exhibit a better self-sealing property under a high pressure. This phenomenon can be explained by analyzing Eq. (12). It can be seen that the decrease in leak rate caused by the decrease in P_g/P_{in} is not sufficient to compensate for the increase in leak rate caused by the increase in permeability $K(\omega_2)$, which causes the beam seal does not exhibit its self-sealing capacity under high fluid pressure in the pipe.

C. IMPROVEMENT OF BEAM SEAL

The average contact pressure of the secondary seal decreases with the increase of fluid pressure is an irreversible characteristic of the beam seal. Therefore, in order to reduce leakage, we can only take measures to reduce the depressurization ratio P_g/P_{in} more.

According to Eq. (11), reducing the permeability of the primary seal $K(\omega_1)$ can reduce the depressurization ratio. This means that increasing the average contact pressure of the primary seal without changing other parameters is beneficial for improving the sealing performance of beam seal under higher fluid pressure. Therefore, we can increase the average

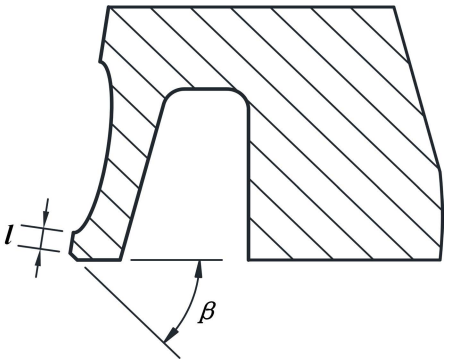

FIGURE 16. Modification with β=80°, l=0.15mm; prototype with β=0°, l=0.57mm.

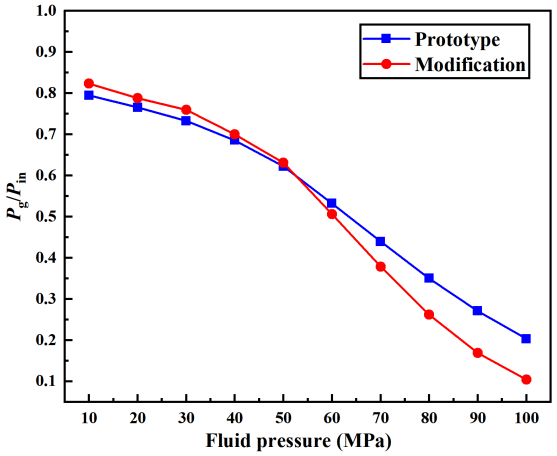

FIGURE 17. Depressurization ratio versus fluid pressure for prototype and modification.

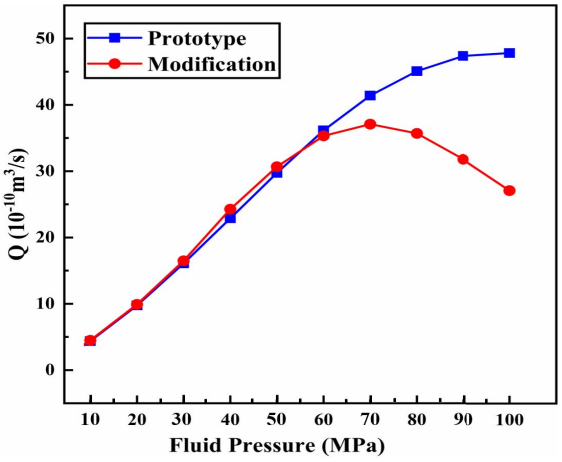

FIGURE 18. Leak rate versus fluid pressure for prototype and modification.

contact pressure by reducing the nominal contact width of primary seal, and the modification is depicted in Fig.16.

Fig.17 and Fig.18 demonstrate the comparison of the depressurization ratio and leak rate between the prototype and modification.

In the pressure range of 10 ∼ 50MPa, the depressurization ratio of the modification is slightly higher than that of the prototype, and after more than 60MPa, the depressurization ratio of the modification is lower than that of the prototype gradually. In particular, with the increase of fluid pressure, the leakage of the modification begins to gradually decrease after the corresponding 60MPa. The result indicates that the reduction of nominal contact width of the primary seal can improve the sealing performance of the beam seal. At the same time, it validates that the beam seal has self-sealing capacity under high fluid pressure in the pipe.

VI. CONCLUSION

This paper presents a novel model to evaluate the leakage performance of a beam seal with two annular sealing areas. The model is obtained on the basis of microscopic porous media analysis of sealing interface and macroscopic finite element analysis of beam seals.

A test rig for measuring the true contact widths of the two sealing areas for the beam seal is established, and the finite element simulation are in good agreement with the experimental results. The two sealing areas and groove form an isolated sealing system, which reduces the fluid pressure driving leakage and improves sealing performance of beam seal. According to the leakage model of the beam seal, reducing roughness of the contact surface and increasing the applied preload can improve the sealing performance of beam seal.

Fluid pressure exerts pressing force on the primary seal increasing the contact force of primary seal, which is beneficial to improve the sealing performance of the beam seal. However, fluid pressure can reduce the contact force of the secondary seal and weaken the sealing performance of the secondary seal. Meanwhile, the depressurization ratio of the beam seal is inversely proportional to fluid pressure. By using the leakage model to analyze the sealing mechanism of beam seal, the sealing performance of beam seal can be improved by setting chamfering in the primary seal. The modification scheme of beam seal is worked out. The calculation shows that the modified beam seal has self-sealing ability compared with its prototype.

The model established in this paper provides a set of methods for quantitative evaluation of sealing performance for beam seal. At the same time, this research lays a foundation for further experimental verification and optimization design of beam seal.

REFERENCES

[1] *SAE Fitting, Tube, Fluid Systems, Separable, Beam Seal*, document 3000/4000 Psi, General Specification for, AS85421A, 2007.

[2] *SAE Fitting, Tube, Fluid Systems, Separable, High pressure Dynamic Beam Seal*, document 5000/8000 Psi, General Specification for, AS85720A, 2008.

[3] *SAE Fitting End Assembly, Internal Thread, Retained Nut, Beam Seal*, document AS4209C, 2019.

[4] *SAE Fittings, Tube, Fluid Systems, Separable, Beam Seal*, document 3000/4000psi, General Specification for, AS854201A, 2007.

[5] *SAE Fittings, Tube, Fluid Systems, Separable, High Pressure Dynamic Beam Seal*, document 5000/8000psi, General Specification for, AS85720A, 2008.

[6] C. J. Liao, H. Chen, H. Lu, R. Dong, H. Sun, and X. Chang, "A leakage model for a seal-on-seal structure based on porous media method," *Int. J. Pressure Vessels Piping*, vol. 188, pp. 1–9, Sep. 2020, doi: 10.1016/j.ijpvp.2020.104227.
[7] B. N. J. Persson, O. Albohr, C. Creton, and V. Peveri, "Contact area between a viscoelastic solid and a hard, randomly rough, substrate," *J. Chem. Phys.*, vol. 120, no. 18, pp. 8779–8793, May 2004, doi: 10.1063/1.1697376.
[8] B. N. J. Persson, N. Prodanov, B. A. Krick, N. Rodriguez, N. Mulakaluri, W. G. Sawyer, and P. Mangiagalli, "Elastic contact mechanics: Percolation of the contact area and fluid squeeze-out," *Eur. Phys. J. E*, vol. 35, no. 1, pp. 1–17, Jan. 2012, doi: 10.1140/epje/i2012-12005-2.
[9] B. Lorenz and B. N. J. Persson, "Leak rate of seals: Effective-medium theory and comparison with experiment," *Eur. Phys. J. E*, vol. 31, no. 2, pp. 159–167, Mar. 2010, doi: 10.1140/epje/i2010-10558-6.
[10] A. G. Akulichev, A. T. Echtermeyer, and B. N. J. Persson, "Interfacial leakage of elastomer seals at low temperatures," *Int. J. Pressure Vessels Piping*, vol. 160, pp. 14–23, Feb. 2018, doi: 10.1016/j.ijpvp.2017.11.014.
[11] F. Bottiglione, G. Carbone, and G. Mantriota, "Fluid leakage in seals: An approach based on percolation theory," *Tribol. Int.*, vol. 42, no. 5, pp. 731–737, May 2009, doi: 10.1016/j.triboint.2008.10.002.
[12] M. Kazeminia and A.-H. Bouzid, "Leak prediction through porous compressed packing rings: A comparison study," *Int. J. Pressure Vessels Piping*, vol. 166, pp. 1–8, Sep. 2018, doi: 10.1016/j.ijpvp.2018.07.012.
[13] S. Jianjun, M. Chenbo, L. Jianhua, and Y. Qiuping, "A leakage channel model for sealing interface of mechanical face seals based on percolation theory," *Tribol. Int.*, vol. 118, pp. 108–119, Feb. 2018, doi: 10.1016/j.triboint.2017.09.013.
[14] X. Ni, C. Ma, J. Sun, Y. Zhang, and Q. Yu, "A leakage model of contact mechanical seals based on the fractal theory of porous medium," *Coatings*, vol. 11, no. 1, pp. 2–18, 2020, doi: 10.3390/coatings11010020.
[15] Q. Zhang, X. Chen, Y. Huang, and Y. Chen, "Fractal modeling of fluidic leakage through metal sealing surfaces," *AIP Adv.*, vol. 8, Apr. 2018, Art. no. 045310, doi: 10.1063/1.5023708.
[16] Q. Zhang, X. Chen, Y. Huang, and X. Zhang, "An experimental study of the leakage mechanism in static seals," *Appl. Sci.*, vol. 1404, no. 8, pp. 1–15, Aug. 2018, doi: 10.3390/app8081404.
[17] A. Majumdar and C. L. Tien, "Fractal characterization and simulation of rough surfaces," *Wear*, vol. 136, no. 2, pp. 313–327, Aug. 1989, doi: 10.1016/0043-1648(90)90154-3.
[18] Y. Zhao, D. M. Maietta, and L. Chang, "An asperity microcontact model incorporating the transition from elastic deformation to fully plastic flow," *J. Tribol.*, vol. 122, no. 1, pp. 86–93, Jan. 2000, doi: 10.1115/1.555332.

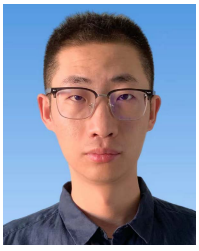

YINGJIA YU received the B.S. and M.S. degrees in engineering mechanics from Liaoning Technical University, China, in 2013 and 2017, respectively. He is currently pursuing the Ph.D. degree with the Marine Engineering College, Dalian Maritime University, China. His research interests include contact mechanics and mechanical seals.

YING CUI received the B.S. degree in thermal engine and the M.S. and Ph.D. degrees in power machinery and engineering from the Harbin Institute of Technology, Harbin, Heilongjiang, China, in 1999, 2001, and 2007, respectively.

From 2005 to 2013, she was a Lecturer with the School of Energy Science and Engineering, Harbin Institute of Technology. Since 2013, she has been an Associate Professor with the Naval Architecture and Ocean Engineering College, Dalian Maritime University. Her research interests include the engine structural strength and vibration, nonlinear rotor dynamics and fault diagnosis, bearing and squeeze film damper dynamics, and piping joint structure design. She has published many academic papers and holds patents in her research field.

Dr. Cui serves as the Executive Director of the Rotor Dynamics Engineering Committee of the Chinese Society of Vibration Engineering.

HONGXIANG ZHANG received the B.S. degree from the Wuhan University of Science and Technology, in 2020. He is currently pursuing the M.S. degree in energy and power engineering with Dalian Maritime University. His research interests include the sealing performance analysis and the structural optimization of beam seal.

DAWEI WANG received the B.S. degree from Dalian Maritime University, in 2021, where he is currently pursuing the M.S. degree in energy and power engineering. His research interests include the sealing performance analysis and the structural design of beam seal.

JINGJUN ZHONG received the B.S. and M.S. degrees in solid rocket engine from Northwestern Polytechnical University, China, in 1985 and 1988, respectively, and the Ph.D. degree in thermal turbomachinery from the Harbin Institute of Technology, China, in 1996.

He is currently the Director of the Institute of Ship Power Engineering, Shanghai Maritime University, China. His research interests include the aerothermodynamics of engines, marine gas turbine technology, marine power plants and systems, marine multi-electric propulsion technology, pressurized maneuvering blade tip winglet technology, and combined engines.